

# Description of the low-mass meson-like spectrum in non-perturbative QCD

Tochtli Yépez-Martínez<sup>1</sup>, Peter O. Hess<sup>2,3</sup> and Osvaldo Civitarese<sup>4</sup>

<sup>1</sup> Instituto de Educación Media Superior de la Ciudad de México, Plantel General Lázaro Cárdenas del Río, Av. Jalalpa Norte 120, Colonia Jalalpa El Grande, C.P. 01377, Alcaldía Alvaro Obregón, Ciudad de México, México.

<sup>2</sup> Instituto de Ciencias Nucleares, Universidad Nacional Autónoma de México, Ciudad Universitaria, Circuito Exterior S/N, A.P. 70-543, 04510 M'exico D.F. Mexico.

<sup>3</sup> Frankfurt Institute for Advanced Studies, J. W. von Goethe University, Hessen, Germany.

<sup>4</sup> Departamento de Física, Universidad Nacional de La Plata, C.C. 67 (1900), La Plata, Argentina, and IFLP-CONICET.

E-mail: [tochtlicuauhtli.yepez@iemss.edu.mx](mailto:tochtlicuauhtli.yepez@iemss.edu.mx), [hess@nucleares.unam.mx](mailto:hess@nucleares.unam.mx), [osvaldo.civitarese@fisica.unlp.edu.ar](mailto:osvaldo.civitarese@fisica.unlp.edu.ar)

**Abstract.** In this work we shall explore the identification and use of effective degrees of freedom, for the description of the non-perturbative regime of QCD. The starting Hamiltonian is the effective Coulomb plus linear potential. In order to build the spectrum of effective quark degrees of freedom, starting from arbitrary chosen quark masses, we shall pre-diagonalized the Hamiltonian. Then, we shall include quark-pair correlations and treat them by applying Bogoliubov transformations. The resulting quasiparticle excitations are then used to construct non-interacting two quasi-quark states with energies up to 2 GeV, which are compared to the observed meson-like states in the same energy domain.

## 1. Introduction

The Quantum Chromodynamics (QCD) is the theory of strong interactions [1, 2, 3], its low energy regime is non-perturbative and in consequence one is forced to apply certain approximations in order to describe hadronic states. Thus the efforts focus in the construction of effective, low-energy approximations to QCD and to find out methods to describe its non-perturbative domain. In this work we investigate the properties of a phenomenological model inspired by the canonical approach to QCD in the physical, Coulomb gauge quantization.

The underlying interactions in Coulomb gauge are dominated by the Instantaneous Color Coulomb Interaction (ICCI) acting between color charges. It has been shown in [4, 5, 6, 7] that the ICCI becomes confining, *i.e.*, proportional to the distance between the external color charges. Beyond the effective quark and antiquark spectrum, the correlations between quark-antiquark pairs lead to meson-like excitations which may be treated as a many-body problem.

In hadronic models, such approximations are driven by phenomenological considerations rather than by QCD itself. Examples of these are the bag model [8, 9], the algebraic models [10, 11, 12, 13] and the constituent-quark model [14]. For these models a number of experimental data points should be considered in order to fit their parameters.

The QCD Hamiltonian in the Coulomb gauge, is a good starting point for the application of many body techniques [15, 16]. The harmonic oscillator basis allows not only to obtain analytic expressions for matrix elements, as shown in [17, 18], but also helps to reduce the size of the matrix to be diagonalized. A cut-off in the harmonic oscillator basis is related to the maximal number of oscillator quanta included in the calculations. The use of the oscillator basis introduces a new way to describe hadrons as a combination of discrete states. This new approach requires another way of performing the renormalization of running constituent quark masses and of the interaction constant. By looking at correlations between pairs of quarks which may result in a superfluid low energy regime, the observed spectrum of hadrons could be interpreted in terms of quasiparticle excitations. This is the purpose of the present work.

In Section 2, we proceed gradually by treating the QCD Hamiltonian in the Coulomb gauge in order to construct the effective quark spectrum. In Section 3, we apply the BCS transformations and solve the corresponding flavor dependent equations, in order to get the relevant parameters of the model, that is the up/down and strange quasi-quark energies and gaps. In Section 4, we present the dependence of the solutions in terms of the dimension of the basis. The conclusions are drawn in Section 5.

## 2. Quarks and antiquarks as effective degrees of freedom.

The first step for the implementation of the BCS method consists in the definition of the single particle field. In the case of QCD the literature is rich in the description of such fields [19, 20, 21, 22, 23, 24, 25, 17].

### 2.1. The QCD Hamiltonian in the Coulomb gauge.

We start from the QCD Hamiltonian in its canonical Coulomb gauge representation [3, 2],

$$\begin{aligned} \mathbf{H}^{QCD} = & \int \left\{ \frac{1}{2} [\mathcal{J}^{-1} \mathbf{\Pi}^{tr} \cdot \mathcal{J} \mathbf{\Pi}^{tr} + \mathcal{B} \cdot \mathcal{B}] - \bar{\psi} (-i\gamma \cdot \nabla + m) \psi - g \bar{\psi} \gamma \cdot A \psi \right\} d\mathbf{x} \\ & + \frac{1}{2} g^2 \int \mathcal{J}^{-1} \rho^c(\mathbf{x}) \langle c, \mathbf{x} | \frac{1}{\nabla \cdot \mathcal{D}} (-\nabla^2) \frac{1}{\nabla \cdot \mathcal{D}} | c' \mathbf{y} \rangle \mathcal{J} \rho^{c'}(\mathbf{y}) d\mathbf{x} d\mathbf{y} , \end{aligned} \quad (1)$$

which has been widely studied in the past for the description of several properties of QCD at low energy [4, 5, 6, 7, 26, 27, 28, 29, 30, 31, 32]. The last term in the Hamiltonian of Eq. (1) includes the relevant interactions between quarks and gluons *i.e.*, the *QCD Instantaneous color-Coulomb Interaction* (QCD-IcCI). At low energy the effects of dynamical gluons in the QCD-IcCI can be represented by the interaction  $V(|\mathbf{x} - \mathbf{y}|) = -\frac{V_C}{|\mathbf{x} - \mathbf{y}|} + V_L |\mathbf{x} - \mathbf{y}|$ , which is obtained from a self-consistent treatment of the interaction between color charge-densities [5, 6].

Here, we have analysed the quark sector of the Hamiltonian of Eq. (1) and taken the effective confining interaction  $V(|\mathbf{x} - \mathbf{y}|)$  to describe the low energy interaction between color charge densities. We write

$$\begin{aligned} \mathbf{H}_{eff}^{QCD} = & \int \left\{ \psi^\dagger(\mathbf{x}) (-i\alpha \cdot \nabla + \beta m) \psi(\mathbf{x}) \right\} d\mathbf{x} - \frac{1}{2} \int \rho_c(\mathbf{x}) V(|\mathbf{x} - \mathbf{y}|) \rho^c(\mathbf{y}) d\mathbf{x} d\mathbf{y} \\ = & \mathbf{K} + \mathbf{H}_{Coul} , \end{aligned} \quad (2)$$

where  $\rho^c(\mathbf{x}) = \psi^\dagger(\mathbf{x}) T^c \psi(\mathbf{x})$  is the quark and antiquark charge-density and  $T^c(T_c)$  are the SU(3) color generators, because of the non-abelian structure of QCD. The first term in Eq. (2) is the kinetic energy, and the second term is the QCD-IcCI in its simplified form. The fermion field  $\psi^\dagger(\mathbf{x})$ , whose quantization is expanded in terms of creation and annihilation operators in the harmonic oscillator basis

$$\psi^\dagger(\mathbf{x}) = \sum_{Nlm_l, \sigma CF} R_{Nl}^*(x) Y_{lm_l}^*(\hat{\mathbf{x}}) \chi_\sigma^\dagger \left( \mathbf{q}_{\frac{1}{2}, Nlm_l, \sigma CF}^\dagger + \mathbf{q}_{-\frac{1}{2}, Nlm_l, \sigma CF}^\dagger \right). \quad (3)$$

with  $x = |\mathbf{x}|$  and  $R_{Nl}(x) = N_{Nl} \exp(-\frac{B_0 x^2}{2}) x^l L_{\frac{N-l}{2}}^{l+\frac{1}{2}}(B_0 x^2)$ , where  $L_n^\lambda$  is an associated Laguerre polynomial and  $(\sqrt{B_0})^{-1}$  is the oscillator length. The index  $\tau$  denotes upper ( $\tau = \frac{1}{2}$ ) and lower ( $\tau = -\frac{1}{2}$ ) components of the Dirac spinors in the Dirac-Pauli representation of the Dirac matrices, and  $\sigma, C, F$  denote spin, color and flavor intrinsic degrees of freedom, respectively.

The use of the harmonic oscillator basis requires the diagonalization of the kinetic term (2), which is performed by using the total spin  $J = l \pm \frac{1}{2}$ , for a given maximal number of quanta  $N = N_{\text{cut}}$ . For this, we introduce a general transformation to a basis of effective operators,

$$\mathbf{q}_{\tau(Nl)JM_JCF}^\dagger = \sum_{\lambda\pi k} \left( \alpha_{\tau(Nl), \lambda\pi k}^{J,T} \right)^* \mathbf{Q}_{\lambda\pi k JM_JCF}^\dagger \delta_{\pi, (-1)^{\frac{1}{2} - \tau + l}}. \quad (4)$$

where the value  $\lambda = +\frac{1}{2}$  will refer to effective quarks and the value  $\lambda = -\frac{1}{2}$  to effective antiquarks, i.e.  $\mathbf{Q}_{\frac{1}{2}\pi k JM_JCF}^\dagger \rightarrow \mathbf{b}_{\pi k JC(Y,T), M_J M_C M_T}^\dagger$  and  $\mathbf{Q}_{-\frac{1}{2}\pi k JM_JCF}^\dagger \rightarrow \mathbf{d}_{\pi k JC(Y,T), M_J M_C M_T}^\dagger$ .

With the use of the harmonic oscillator basis and the pre.-diagonalization of the kinetic term, we have identified effective quarks and antiquarks as a linear combinations of the bare quarks and antiquarks. In terms of these effective quarks and antiquarks, the kinetic energy term acquires the following structure

$$K = \sum_{k\pi\gamma} \varepsilon_{k\pi\gamma} \sum_\mu \left( \mathbf{b}_{k\pi\gamma\mu}^\dagger \mathbf{b}^{k\pi\gamma\mu} - \mathbf{d}_{k\pi\gamma\mu}^\dagger \mathbf{d}^{k\pi\gamma\mu} \right), \quad (5)$$

The indices indicate the principal number ( $k = 1, 2, \dots$ ) which run over all orbital states and the parity ( $\pi = \pm$ ) while  $\gamma, \mu$  are short hand notation for the particle spin, color and flavor hypercharge and isospin representations  $\gamma = \{J, C, (Y, T)\}$  and their magnetic projections  $\mu = \{M_J, M_C, M_T\}$ , respectively.

The QCD-IcCI term, in its simplified form ( $\mathbf{H}_{\text{Coul}}$ ), rewritten in terms of effective quarks and antiquarks operators is given by [18]

$$\begin{aligned} \mathbf{H}_{\text{Coul}} = & - \frac{1}{2} \sum_L \sum_{\lambda_i \mathbf{q}_i} V_{\{\lambda_i \mathbf{q}_i\}}^L \left( \left[ \mathcal{F}_{\lambda_1 \mathbf{q}_1, \lambda_2 \mathbf{q}_2; \gamma_{f_0}} \mathcal{F}_{\lambda_3 \mathbf{q}_3, \lambda_4 \mathbf{q}_4; \bar{\gamma}_{f_0}} \right]_{\mu_0}^{\gamma_0} + \left[ \mathcal{F}_{\lambda_1 \mathbf{q}_1, \lambda_2 \mathbf{q}_2; \gamma_{f_0}} \mathcal{G}_{\lambda_3 \mathbf{q}_3, \lambda_4 \mathbf{q}_4; \bar{\gamma}_{f_0}} \right]_{\mu_0}^{\gamma_0} \right. \\ & \left. + \left[ \mathcal{G}_{\lambda_1 \mathbf{q}_1, \lambda_2 \mathbf{q}_2; \gamma_{f_0}} \mathcal{F}_{\lambda_3 \mathbf{q}_3, \lambda_4 \mathbf{q}_4; \bar{\gamma}_{f_0}} \right]_{\mu_0}^{\gamma_0} + \left[ \mathcal{G}_{\lambda_1 \mathbf{q}_1, \lambda_2 \mathbf{q}_2; \gamma_{f_0}} \mathcal{G}_{\lambda_3 \mathbf{q}_3, \lambda_4 \mathbf{q}_4; \bar{\gamma}_{f_0}} \right]_{\mu_0}^{\gamma_0} \right) \end{aligned} \quad (6)$$

where we have compacted the single particle orbital number, parity and irreps into the short-hand notation  $\mathbf{q}_i = k_i \pi_{q_i} \gamma_{q_i}$ , and use for the (flavor-less) quantum numbers of the intermediate coupling in the interaction  $\gamma_{f_0} = \{L(11)(0, 0)\}$  and for their magnetic projections  $\mu_{f_0} = \{M_L, M_C, 0\}$ . The conjugate representations satisfy  $\bar{\gamma}_{f_0} = \gamma_{f_0}$  and  $\bar{\mu}_{f_0} = \{-M_L, M_C, 0\}$ . For the total couplings (upper index) and magnetic numbers (lower index) of the interaction, we have used  $\gamma_0 = \{0, (00), (0, 0)\}$  and  $\mu_0 = \{0, 0, 0\}$  respectively. The operators  $\mathcal{F}$  and  $\mathcal{G}$  are given by

$$\begin{aligned} \mathcal{F}_{\lambda_1 \mathbf{q}_1, \lambda_2 \mathbf{q}_2; \gamma_{f_0}, \mu_{f_0}} &= \frac{1}{\sqrt{2}} \left\{ \delta_{\lambda_1, \frac{1}{2}} \delta_{\lambda_2, \frac{1}{2}} \left[ \mathbf{b}_{\mathbf{q}_1}^\dagger \otimes \mathbf{b}_{\bar{\mathbf{q}}_2} \right]_{\mu_{f_0}}^{\gamma_{f_0}} - \delta_{\lambda_1, -\frac{1}{2}} \delta_{\lambda_2, -\frac{1}{2}} \left[ \mathbf{d}_{\bar{\mathbf{q}}_1}^\dagger \otimes \mathbf{d}_{\mathbf{q}_2}^\dagger \right]_{\mu_{f_0}}^{\gamma_{f_0}} \right\} \\ \mathcal{G}_{\lambda_1 \mathbf{q}_1, \lambda_2 \mathbf{q}_2; \gamma_{f_0}, \mu_{f_0}} &= \frac{1}{\sqrt{2}} \left\{ \delta_{\lambda_1, -\frac{1}{2}} \delta_{\lambda_2, \frac{1}{2}} \left[ \mathbf{d}_{\mathbf{q}_1}^\dagger \otimes \mathbf{b}_{\bar{\mathbf{q}}_2} \right]_{\mu_{f_0}}^{\gamma_{f_0}} - \delta_{\lambda_1, \frac{1}{2}} \delta_{\lambda_2, -\frac{1}{2}} \left[ \mathbf{b}_{\mathbf{q}_1}^\dagger \otimes \mathbf{d}_{\bar{\mathbf{q}}_2}^\dagger \right]_{\mu_{f_0}}^{\gamma_{f_0}} \right\}. \end{aligned} \quad (7)$$

In this basis, and using the above introduced states, the matrix elements of the interaction are given by

$$\begin{aligned} V_{\{\lambda_i \pi_i k_i J_i Y_i T_i\}}^L &= \sum_{\tau_i N_i l_i} V_{\{N_i l_i J_i\}}^L \alpha_{\tau_1(N_1 l_1), \lambda_1, \pi_1, k_1}^{J_1, T_1} \alpha_{\tau_2(N_2 l_2), \lambda_2, \pi_2, k_2}^{J_2, T_2} \alpha_{\tau_3(N_3 l_3), \lambda_3, \pi_3, k_3}^{J_3, T_3} \alpha_{\tau_4(N_4 l_4), \lambda_4, \pi_4, k_4}^{J_4, T_4} \\ &\times \delta_{\tau_1 \tau_2} \delta_{\tau_3 \tau_4} \delta_{\pi_1, (-1)^{\frac{1}{2} - \tau_1 + l_1}} \delta_{\pi_2, (-1)^{\frac{1}{2} - \tau_2 + l_2}} \delta_{\pi_3, (-1)^{\frac{1}{2} - \tau_3 + l_3}} \delta_{\pi_4, (-1)^{\frac{1}{2} - \tau_4 + l_4}} \\ &\times (-1)^{\frac{1}{3} + \frac{Y_1}{2} + T_1} \frac{\sqrt{2T_1 + 1}}{\sqrt{3}} \delta_{T_2 T_1} \delta_{Y_2 Y_1} (-1)^{\frac{1}{3} + \frac{Y_3}{2} + T_3} \frac{\sqrt{2T_3 + 1}}{\sqrt{3}} \delta_{T_4 T_3} \delta_{Y_4 Y_3}. \end{aligned} \quad (8)$$

The matrix elements in the harmonic oscillator basis ( $V_{\{N_i l_i J_i\}}^L$ ) are analytic and actually easy to compute.

### 3. Bogoliubov Transformation and the BCS method.

Here, starting from the effective quark and antiquarks basis, we apply the *Bogoliubov Transformation* [15, 16], in order to approximately diagonalize part of the effective QCD interaction, Eq. (2).

Herewith we shall apply the transformations for each quark-flavor, separately. Thus, the reference (ground state) state will be a quark condensate with a definite flavor. Then, the Hamiltonian of Eq.(2) is written in terms of quasi-quark operators and the standard conditions of the BCS theory are applied to it by asking the one-quasiparticle term ( $H_{11}$ ) to be diagonal, the pairs terms ( $H_{20} + H_{02}$ ) to vanish. A crucial step in the treatment, leading to the transformation between ordinary particles (in this case fermions like the quarks and antiquarks) to quasiparticles is the replacement of the ordinary vacuum  $|0\rangle$  by the BCS vacuum  $|BCS\rangle$ ,

$$|BCS\rangle \sim |0\rangle + \sum_{k_1 \pi_1 \gamma_1} z_{k_1 \pi_1 \gamma_1} \left[ \mathbf{b}_{k_1 \pi_1 \gamma_1}^\dagger \otimes \mathbf{d}_{k_1 \pi_1 \bar{\gamma}_1}^\dagger \right]_{\mu_0}^{\gamma_0} |0\rangle \quad (9)$$

The quasiparticle excitation  $\mathbf{B}_{k_i \pi_i, \gamma_i \mu_i}^\dagger |BCS\rangle$  operator has the quantum numbers of the quark, and the quasiparticle excitation  $\mathbf{D}_{k_i \pi_i, \gamma_i \mu_i}^\dagger |BCS\rangle$  operator has the quantum numbers of the antiquark, being  $\mathbf{B}_{k_i \pi_i, \gamma_i \mu_i}^\dagger$  and  $\mathbf{D}_{k_i \pi_i, \gamma_i \mu_i}^\dagger$  the creation operators for quasi-quarks and quasi-antiquarks, respectively.

At the same time the following conditions:

$$\mathbf{B}^{k_i \pi_i, \gamma_i \mu_i} |BCS\rangle = \mathbf{D}_{k_i \pi_i, \gamma_i \mu_i} |BCS\rangle = 0, \quad (10)$$

$$\left\{ \mathbf{B}^{k_i \pi_i, \gamma_i \mu_i}, \mathbf{B}_{k_j \pi_j, \gamma_j \mu_j}^\dagger \right\} = \left\{ \mathbf{D}_{k_i \pi_i, \gamma_i \mu_i}, \mathbf{D}^{\dagger k_j \pi_j, \gamma_j \mu_j} \right\} = \delta_{ij} \quad (11)$$

and

$$\left\{ \mathbf{B}^{k_i \pi_i, \gamma_i \mu_i}, \mathbf{D}^{\dagger k_j \pi_j, \gamma_j \mu_j} \right\} = \left\{ \mathbf{B}^{k_i \pi_i, \gamma_i \mu_i}, \mathbf{D}_{k_i \pi_i, \gamma_i \mu_i} \right\} = 0 \quad (12)$$

should be obeyed.

The next step in our derivation consists of taking normal order respect to the quasiparticle vacuum and collecting the different contributions to the Hamiltonian with constant terms  $H_{00}$ , one creation-one annihilations terms  $H_{11}$ , two-quasiparticle terms  $H_{20}$  and  $H_{02}$ .

The value of the gap is extracted, for each channel, by solving the set of BCS equations (see Section 3.1) and the remanent of the transformed Hamiltonian may be treated in the RPA basis to describe correlations between pairs of quasiparticles [33].

### 3.1. BCS equations.

The terms  $H_{11}$  and  $H_{20} + H_{02}$  can be ordered in terms of the following variables

$$\begin{aligned} X_{k_1} &= u_{k_1}^2 - v_{k_1}^2 \\ Y_{k_1} &= 2u_{k_1}v_{k_1} \end{aligned} \quad (13)$$

which depend only on the quasiparticle operator indices,  $k_i$ . Here, we are using a short-hand notation  $k_i = k_i \pi_i, \gamma_i$ . The interaction terms are also ordered in terms of the structures  $(u_{k_2}^2 - v_{k_2}^2)$  and  $(u_{k_2}v_{k_2})$ , being  $k_2$  an internal index. The parameters  $u_k$  and  $v_k$  are determined self-consistently.

The resulting equations are the well known BCS-equations

$$\Sigma_{k_1} X_{k_1} + \Delta_{k_1} Y_{k_1} = E_{k_1} \quad (14)$$

$$-\Delta_{k_1} X_{k_1} + \Sigma_{k_1} Y_{k_1} = 0 \quad (15)$$

where  $\Sigma_{k_1}$ ,  $\Delta_{k_1}$  and the quasiparticle energy  $E_{k_1}$  are given by

$$\Sigma_{k_1} = \varepsilon_{k_1} + \bar{V}_{k_1 k_2 k_2 k_1}^{\Sigma} (u_{k_2}^2 - v_{k_2}^2) \quad (16)$$

$$\begin{aligned} \Delta_{k_1} &= \bar{V}_{k_1 k_2 k_2 k_1}^{\Delta} (u_{k_2} v_{k_2}) \\ E_{k_1} &= \sqrt{\Sigma_{k_1}^2 + \Delta_{k_1}^2} \end{aligned} \quad (17)$$

with

$$\begin{aligned} &\bar{V}_{k_1 \pi_1 J_1 Y_1 T_1, k_2 \pi_2 J_2 Y_2 T_2, k_2 \pi_2 J_2 Y_2 T_2, k_1 \pi_1 J_1 Y_1 T_1}^{\Sigma} = \\ &-\frac{1}{2} \sum_L \sum_{\lambda_i} \left( \frac{1}{2} \right) \frac{\sqrt{8(2L+1)}}{9} \frac{(-1)^{L+J_2-J_1}}{2J_1+1} \\ &\times \left\{ \sum_{\tau_i N_i l_i} V_{\{N_i l_i J_i\}}^L \alpha_{\tau_1(N_1 l_1), \lambda_1, \pi_1, k_1}^{J_1, T_1} \alpha_{\tau_2(N_2 l_2), \lambda_2, \pi_2, k_2}^{J_2, T_2} \alpha_{\tau_3(N_3 l_3), \lambda_3, \pi_3, k_3}^{J_3, T_3} \alpha_{\tau_4(N_4 l_4), \lambda_4, \pi_4, k_4}^{J_4, T_4} \right. \\ &\times \delta_{\tau_1 \tau_2} \delta_{\tau_3 \tau_4} \delta_{\pi_1, (-1)^{\frac{1}{2}-\tau_1+l_1}} \delta_{\pi_2, (-1)^{\frac{1}{2}-\tau_2+l_2}} \delta_{\pi_3, (-1)^{\frac{1}{2}-\tau_3+l_3}} \delta_{\pi_4, (-1)^{\frac{1}{2}-\tau_4+l_4}} \left. \right\} \\ &\times (\delta_{\pi_1 \pi_4}) (\delta_{k_2 k_3} \delta_{\pi_2 \pi_3}) (\delta_{J_2 J_3} \delta_{J_1 J_4}) (\delta_{T_1 T_2} \delta_{T_2 T_3} \delta_{T_3 T_4}) (\delta_{Y_1 Y_2} \delta_{Y_2 Y_3} \delta_{Y_3 Y_4}) \\ &\times (\delta_{\lambda_1 + \frac{1}{2}} \delta_{\lambda_2 + \frac{1}{2}} \delta_{\lambda_3 + \frac{1}{2}} \delta_{\lambda_4 + \frac{1}{2}} - \delta_{\lambda_1 - \frac{1}{2}} \delta_{\lambda_2 + \frac{1}{2}} \delta_{\lambda_3 + \frac{1}{2}} \delta_{\lambda_4 - \frac{1}{2}}) \text{average} \end{aligned} \quad (18)$$

and

$$\begin{aligned} &\bar{V}_{k_1 \pi_1 J_1 Y_1 T_1, k_2 \pi_2 J_2 Y_2 T_2, k_2 \pi_2 J_2 Y_2 T_2, k_1 \pi_1 J_1 Y_1 T_1}^{\Delta} = \\ &-\frac{1}{2} \sum_L \sum_{\lambda_i} \left( \frac{1}{2} \right) \frac{\sqrt{8(2L+1)}}{9} \frac{(-1)^{L+J_2-J_1}}{2J_1+1} \\ &\times \left\{ \sum_{\tau_i N_i l_i} V_{\{N_i l_i J_i\}}^L \alpha_{\tau_1(N_1 l_1), \lambda_1, \pi_1, k_1}^{J_1, T_1} \alpha_{\tau_2(N_2 l_2), \lambda_2, \pi_2, k_2}^{J_2, T_2} \alpha_{\tau_3(N_3 l_3), \lambda_3, \pi_3, k_3}^{J_3, T_3} \alpha_{\tau_4(N_4 l_4), \lambda_4, \pi_4, k_4}^{J_4, T_4} \right. \\ &\times \delta_{\tau_1 \tau_2} \delta_{\tau_3 \tau_4} \delta_{\pi_1, (-1)^{\frac{1}{2}-\tau_1+l_1}} \delta_{\pi_2, (-1)^{\frac{1}{2}-\tau_2+l_2}} \delta_{\pi_3, (-1)^{\frac{1}{2}-\tau_3+l_3}} \delta_{\pi_4, (-1)^{\frac{1}{2}-\tau_4+l_4}} \left. \right\} \\ &\times (\delta_{\pi_1 \pi_4}) (\delta_{k_2 k_3} \delta_{\pi_2 \pi_3}) (\delta_{J_2 J_3} \delta_{J_1 J_4}) (\delta_{T_1 T_2} \delta_{T_2 T_3} \delta_{T_3 T_4}) (\delta_{Y_1 Y_2} \delta_{Y_2 Y_3} \delta_{Y_3 Y_4}) \\ &\times 2(\delta_{\lambda_1 + \frac{1}{2}} \delta_{\lambda_2 + \frac{1}{2}} \delta_{\lambda_3 - \frac{1}{2}} \delta_{\lambda_4 - \frac{1}{2}} + \delta_{\lambda_1 - \frac{1}{2}} \delta_{\lambda_2 + \frac{1}{2}} \delta_{\lambda_3 - \frac{1}{2}} \delta_{\lambda_4 + \frac{1}{2}}) , \end{aligned} \quad (19)$$

where the summation on the internal indices is performed.

These non-linear equations are then solved for each of the quark-flavors and they are known as state depended BCS-equations [15, 16], because  $\Sigma_{k_1}$  and  $\Delta_{k_1}$  depend on the flavor.

The procedure to obtain the solutions of Eqs. (14) and (15) consist of the variation of the quantities  $u_{k_i}$  and  $v_{k_i}$ , such that the iteration stop when the correlation energy  $E_{k_1}$  reaches stability.

#### 4. Results and Discussions.

In this section we shall present the results of our calculations. We have considered the effects associated to the renormalization of the parameters, *i.e.*, the quarks masses and the Coulomb and linear interactions. At the same time we have studied the effects of a correlated vacuum and the presence of a gap for each quark flavor by comparing the spectrum of the pre-diagonalization energies with the quasiparticle energies, as a function of the cut-off parameter ( $N_{cut}$ ). At the end of this section, we have constructed the uncorrelated two-quasiparticle spectrum and compared it to the experimental ones [34]. The main aspect of the comparison between calculations and data will focus on the density of states, for which we shall investigate if the space of uncorrelated two-quasiparticle states is dense enough to establish connections with data.

##### 4.1. Renormalization of the parameters.

The renormalization implemented takes into account a cut-off in the number of oscillator quanta  $N_{cut}$ , such a truncation is similar to a momentum cut-off regularization, but in a discrete basis. The aim of the renormalization procedure is to keep at least the lowest eigenvalue of the BCS equations  $E_{k_i}$  unchanged, for each quark flavor. Thus, we present the renormalization results which, in fact, does succeed in keeping the low-energy meson-like spectrum approximately cut-off-independent.

We shall proceed by studying the dependence of the parameters which enter into the definition of the interaction, which are  $V_C$  and  $V_L$ . Fig. 1 shows the dependence of the parameters  $V_C$  and  $V_L$  upon the value of the cutoff,  $N_{cut}$ , of the radial basis. In doing so we have varied both  $V_C$  and  $V_L$  such that the resulting values of the gaps remain constant.

In Fig. 1, it is seen that the strength of the renormalized Coulomb interaction increases as a function of  $N_{cut}$ . This change is faster than the decrease observed in the strength of the renormalized linear interaction.

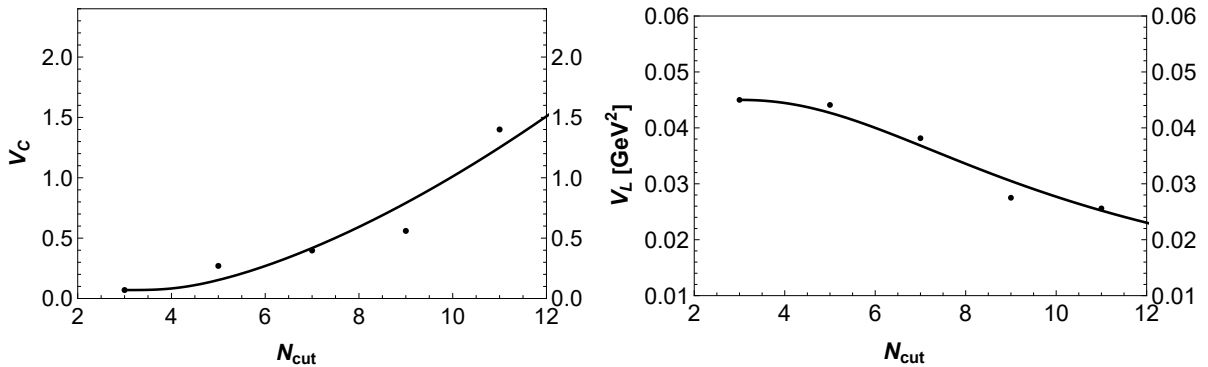


Figure 1: Renormalization of the Coulomb  $V_C$  (left) and linear interaction  $V_L$  (right): dependence of the parameters upon the size of the radial basis ( $N_{cut}$ ). The actual values are represented by dots, the line is to guide the eye. We are using natural units through the text.

For the renormalization of the up/down quark mass  $m_q$ , we have used a starting value of  $m_q = 0.050\text{GeV}$ . In the case of the strange quark mass, we have used the highest value for

which a gap in the strange sector is not zero, this is at about  $m_s = 0.140\text{GeV}$ , for higher values than this, there is no gap in the strange quark sector.

#### 4.2. Quasiparticle spectrum.

Proceeding in the same manner, with the couplings of the previous subsection, we have diagonalized the one quasiparticle sector of the Hamiltonian and solved the BCS equations (14) and (15). The results for the up/down quarks  $T = \frac{1}{2}$  and strange quark  $T = 0$  are shown in Figure 2.

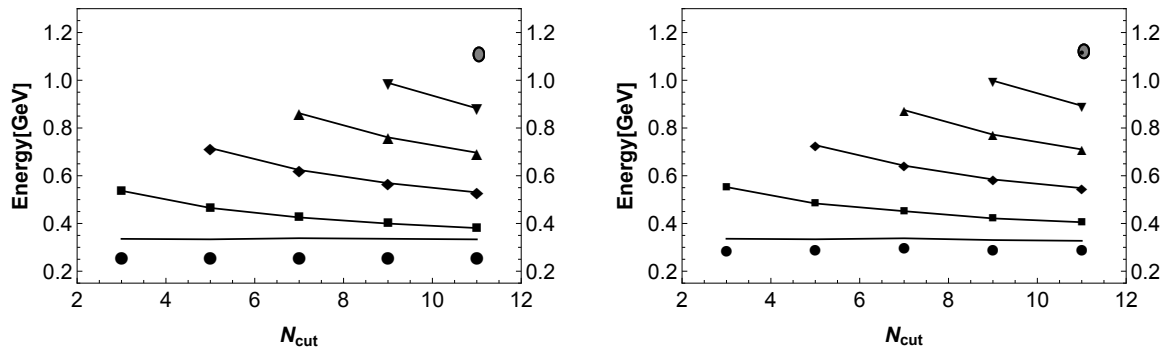


Figure 2: Prediagonalization energies (symbols) for  $T = \frac{1}{2}$  (left) and  $T = 0$  (right) states and Quasiparticle (solid lines) energies versus  $N_{cut}$ .

From the comparison between the energies obtained by diagonalizing the one particle sector of the Hamiltonian and those corresponding to the quasiparticles, we may conclude that in both cases the spectrum reaches a harmonic limit for large values of  $N_{cut}$ . The constancy of the gap for the up/down and strange quarks is well illustrated by the results shown in Figure 2, where the gap in the case of  $T = \frac{1}{2}$  states is  $\Delta \approx 0.2$  GeV and for  $T = 0$  its value is  $\Delta \approx 0.15$  GeV .

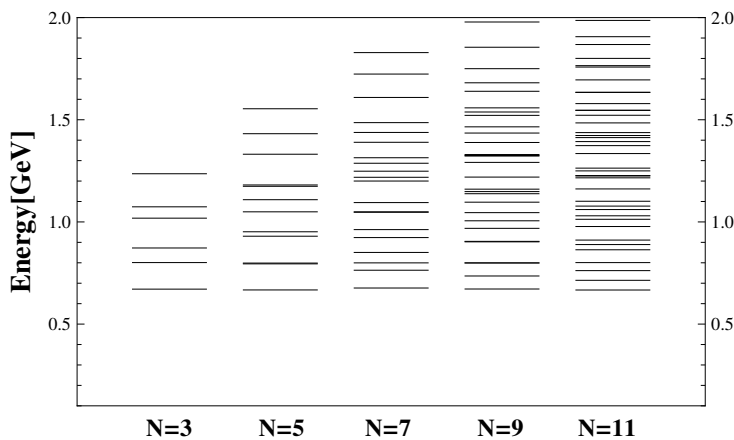


Figure 3: Two-Quasiparticle meson-like spectrum, for pairs of up and down quasiquarks, isospin  $T = 0, 1$  states, vs  $N_{cut}$ .

*4.2.1. Two quasiparticle spectrum as a function of  $N_{cut}$*  Meson states, of positive and negative parities, are described as two-quasiparticle states. In Figure 3 the spectrum of two-quasiparticles, for the subspace  $T = 0, 1$ , is shown as a function of  $N_{cut}$ . The density of states increases as the

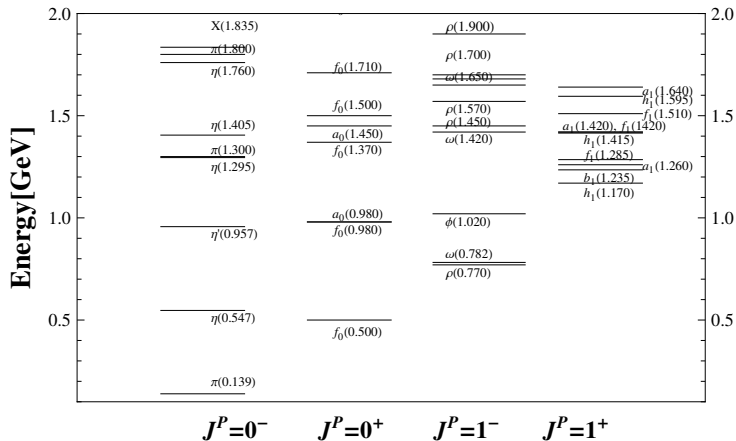


Figure 4: Experimental meson spectrum for isospin  $T = 0, 1$ , up to 2 GeV.

number of states in the basis increases. The density observed for  $N_{cut} = 9, 11$  seems to be similar to that observed in the experimental spectrum shown in Figure 4. The figure is not meant to be compared with data but rather show the gross features of the spectrum. Considering that the theoretical results have been obtained at the quasiparticle level, that is without including residual interactions between pairs of quasiparticles, the overall tendency of them follows that of the experiment. This is particularly true for the sector of medium and high energies. This is encouraging because the addition of the residual terms of the interaction between pairs of quasiparticles, when treated in the context of non-perturbative linearization method, like the RPA approach, could certainly improve the agreement.

## 5. Conclusions.

In this work we have treated the Coulomb plus linear QCD Hamiltonian by applying non-perturbative techniques like the BCS method. A renormalization of the mass and interaction parameters was performed. The stability of the results was tested by increasing the dimension of the radial basis used in the calculations. We have calculated the gaps and quasiparticle energies for up/down and strange sectors. The two-quasiparticle spectrum for  $T = \frac{1}{2}$  and  $T = 0$ , that is mesons and kaons like states, show features similar to those exhibited by the experiments.

It is expected that by including interactions between pairs of quasiparticles, would allow for a more detailed correspondence between theoretical and experimental results. Work is in progress about the use of the RPA methods in this context.

## Acknowledgments

P.O.H. acknowledges financial support from PAPIIT-DGAPA (IN100421). O.C acknowledges the support of the CONICET and of the ANPCyT of Argentina (PIP-616).

- [1] S. Weinberg, *The Quantum Theory of Fields* (Vol. II, Cambridge University Press, 1996).
- [2] T. D. Lee, *Particle Physics and Introduction to Field Theory* (Harwood Academic Publishers, New York, 1981).
- [3] N. H. Christ and T. D. Lee, Phys. Rev. D **22**, 939 (1980).
- [4] A. Szczepaniak, E. S. Swanson, C. R. Ji and S. R. Cotanch, Phys. Rev. Lett. **76**, 2011 (1996).
- [5] A. P. Szczepaniak and E. Swanson, Phys. Rev. D **65**, 025012 (2001).
- [6] C. Feuchter and H. Reinhardt, Phys. Rev. D **70**, 105021 (2004).
- [7] H. Reinhardt, D. R. Campagnari and A. P. Szczepaniak, Phys. Rev. D **84**, 045006 (2011).
- [8] T. DeGrand, R. L. Jaffe, K. Johnson, and J. Kiskis, Phys. Rev. D **12**, 2060 (1975).
- [9] W. Greiner, S. Schramm, and E. Stein, *Quantum Chromodynamics* (Spiriner, Heidelberg, 2002).
- [10] R. Bijker, F. Iachello, and A. Leviatan, Ann. Phys. (NY) **236**, 69 (1994).

- [11] T. Yepez-Martinez, O. Civitarese and P. O. Hess, *Int. J. Mod. Phys. E* **25**, 1650067 (2016).
- [12] T. Yepez-Martinez, O. Civitarese and P. O. Hess, *Int. J. Mod. Phys. E* **26**, 1750012 (2017).
- [13] U. I. Ramirez-Soto, O. A. Rico-Trejo, T. Yépez-Martínez, P. O. Hess, A. Weber and O. Civitarese, *J. Phys. G: Nucl. Part. Phys.* **48**, 085013 (2021).
- [14] N. Isgur and G. Karl, *Phys. Rev. D* **18**, 4187 (1978).
- [15] P. Ring and P. Schuck, *The Nuclear Many Body Problem* (Springer, Heidelberg, 1980).
- [16] A. L. Fetter and J. D. Walecka, *Quantum Theory of Many-Particle Systems* (Dover, New York, 2003).
- [17] T. Yépez-Martínez, P. O. Hess, A. P. Szczepaniak and O. Civitarese, *Phys. Rev. C* **81**, 045204 (2010).
- [18] D. A. Amor-Quiroz, T. Yépez-Martínez, P. O. Hess, O. Civitarese, and A. Weber, *Int. J. Mod. Phys. E* **26**, 1750082 (2017)
- [19] J. R. Finger and J. E. Mandula, *Nucl. Phys.* **B199**, 168 (1982)
- [20] S. L. Adler and A. C. Davis, *Nucl. Phys.* **B244**, 469 (1984)
- [21] A. Le Yaouanc, L. Oliver, O. Pène, and J.-C. Raynal, *Phys. Rev. D* **29**, 1233 (1984)
- [22] P. J. de A. Bicudo and J. E. F. T. Ribeiro, *Phys. Rev. D* **42**, 1611 (1990).
- [23] F. J. Llanes-Estrada and S. R. Cotanch, *Phys. Rev. Lett.* **84**, 1102 (2000).
- [24] F. J. Llanes-Estrada and S. R. Cotanch, *Nucl. Phys. A* **697**, 303 (2002).
- [25] A. V. Nefediev, J. E. F. T. Ribeiro, and A. P. Szczepaniak, *JETP Lett.* **87**, 271 (2008).
- [26] A. P. Szczepaniak and E. S. Swanson, *Phys. Rev. D* **55**, 1578 (1997).
- [27] D. Zwanziger, *Phys. Rev. Lett.* **90**, 102001 (2003).
- [28] J. Greensite and S. Olejnik, *Phys. Rev. D* **67**, 094503 (2003).
- [29] P. Guo, A. P. Szczepaniak, G. Galat'a, A. Vassallo, and E. Santopinto, *Phys. Rev. D* **78**, 056003 (2008)
- [30] T. Yépez-Martínez, A. P. Szczepaniak and H. Reinhardt, *Phys. Rev. D* **86**, 076010 (2012).
- [31] J. Greensite and A. P. Szczepaniak, *Phys. Rev. D* **91**, (2015) 034503.
- [32] J. Greensite and A. P. Szczepaniak, *Phys. Rev. D* **93**, (2016) 074506.
- [33] T. Yépez-Martínez, P. O. Hess and O. Civitarese, work in progress to be published.
- [34] P.A. Zyla et al. (Particle Data Group), *Prog. Theor. Exp. Phys.* **2020**, 083C01 (2020).